

## **Supplementary Materials**

### **Tertiary lymphoid structures induced by CXCL13-producing CD4<sup>+</sup> T cells increase tumor infiltrating CD8<sup>+</sup> T cells and B cells in ovarian cancer**

Masayo Ukita, Junzo Hamanishi, Hiroyuki Toshitomi, Koji Yamanoi, Shiro Takamatsu, Akihiko Ueda, Haruka Suzuki, Yuko Hosoe, Yoko Furutake, Mana Taki, Kaoru Abiko, Ken Yamaguchi, Hidekatsu Nakai, Tukasa Baba, Noriomi Matsumura, Akihiko Yoshizawa, Hideki Ueno, Masaki Mandai

- **Supplementary Methods**
- **Supplementary Table S1-S2**
- **Supplementary Figure S1-S3**

## **Supplementary Methods**

### **Establishment of a patient derived cell line, DK-09**

The patient was diagnosed with peritoneal carcinoma stage IIIB, and the histology indicated high grade serous carcinoma. The patient underwent primary debulking surgery and six cycles of dose-dense paclitaxel/carboplatin as adjuvant chemotherapy. The patient was treated with gemcitabine/carboplatin + bevacizumab and pegylated liposomal doxorubicin after recurrence, but they were ineffective. When cell-free and concentrated ascites reinfusion therapy (CART) was performed for the palliation of symptoms, a sample of ascites was obtained with the patient's informed consent. The cells were collected by centrifugation, lysed with ACK lysing buffer (Cat# 10-548E, LONZA, Basel, Switzerland) to remove red blood cells, and treated with Liberase (37°C for 30 minutes) (Cat# 5401127, Roche, Basel, Switzerland). CD45-MACS beads (Cat# 130-052-301, Miltenyi Biotec) were added and CD45<sup>+</sup> cells were removed by the column method.

Flow cytometry was used to confirm the cells were negative for CD45 after the removal of CD45<sup>+</sup> cells. Anti-fibroblast antibody was used to confirm the absence of fibroblasts. We confirmed that approximately 60% of the cells were positive for FOLR1, which is positive in most ovarian cancers. The cells were then passaged in RPMI + 20% fetal bovine serum, and autonomous growth was observed. In Passage 28 cells, 98.7% of the cells were CD45-negative and 77% of the cells were FOLR1-positive, and these cells were used in subsequent experiments.

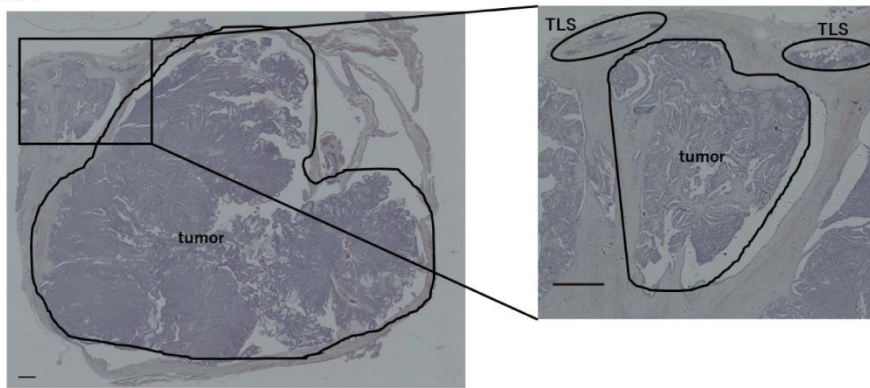
**Supplementary Table S1. Patients' characteristics**

	Kyoto Univ. cohort	Kindai Univ. cohort	Total
Histology	High grade serous carcinoma		
No. of cases	62	35	97
Age (median, years)	56.5	63	60
(range)	(35-82 )	(42-84)	(35-84)
Stage I	7	7	14
Stage II	5	3	8
Stage III	44	17	61
Stage IV	6	8	14
TLS positive cases	39	22	61
( % )	62.9	62.8	62.9
Median follow up (month)	76	52	59
(range)	(8-196)	(1-120)	(1-196)

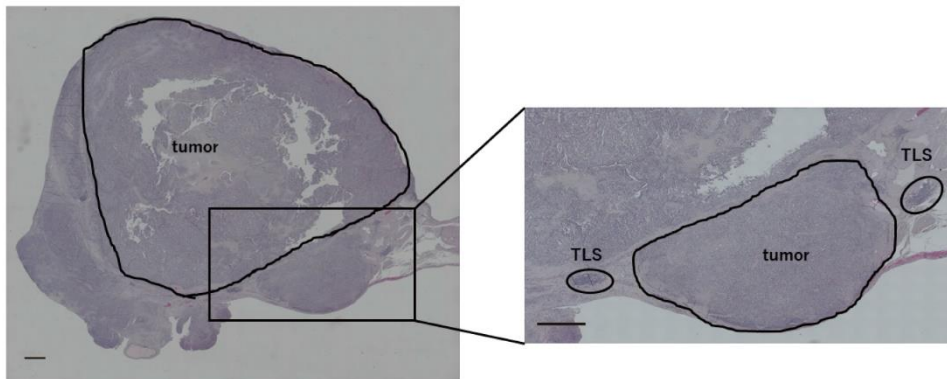
**Supplementary Table S2. Materials used for immunohistochemistry, RNA in situ hybridization, flow cytometry, and ELISA**

<b>Immunohistochemistry</b>	<b>Source</b>	<b>Catalog #</b>
Mouse anti-human CD8 (Clone: C8/144B)	Nichirei Biosciences	413201
Rabbit anti-human CD4 (clone: SP35), 1:100 dilution	Cell Marque	104R-14
Mouse anti-human CD20 (clone: L26), 1:500 dilution	Novus Biologicals	NBP2-44743
Rabbit anti-human CD38 (clone: SP149), 1:100 dilution	Arigo Biolaboratories	ARG52764
Mouse anti-human CD21 (clone: 1F8), 1:10 dilution	Novus Biologicals	NBP1-22527
Rat anti-mouse CD4 (clone: H129.19), 1:200 dilution	BD Pharmingen/BD Biosciences	550278
Rat anti-mouse CD8 (clone: YTS169.4), 1:200 dilution	Abcam	ab22378
Rat anti-mouse CD19 (clone: 6D5), 1:200 dilution	Abcam	ab25232
Rat anti-mouse/human Ki67 (clone: SolA15), 1:100 dilution	Thermo Fisher	14-5698-80
Rabbit anti-mouse CD8 (clone: EPR20305), 1:2000 dilution	Abcam	ab209775
<b>RNA in situ hybridization</b>		
Hs-CXCL13 (for human) (C1)	Advanced Cell Diagnostics	311321
Mm-Cxcl13 (for mouse)	Advanced Cell Diagnostics	406311
Hs-CD4 (C2) (for human)	Advanced Cell Diagnostics	605601-C2
Hs-CD8A (C3) (for human)	Advanced Cell Diagnostics	560391-C3
Hs-CR2 *(C2) (for human)	Advanced Cell Diagnostics	859071-C2
Opal 690, 1:1000 dilution	PerkinElmer	FP1497001KT
Opal 570, 1:1500 dilution	PerkinElmer	FP1488001KT
*Hs-CR2 targeting 269-1303 of NM_001006658.3		
<b>Flow cytometry</b>		
APC-conjugated mouse anti-human CXCL13 (clone: 53610)	R&D Systems	IC801A
BV421-conjugated rat anti-Human CXCR5 (clone: RF8B3)	BD Biosciences	562747
PE-conjugated mouse anti-Human CD279 (clone: EH12.2H7)	BioLegend	329906
<b>ELISA</b>		
Human CXCL13/BLC/BCA-1 Quantikine ELISA Kit	R&D Systems	DCX130
TGFβ-1 Human ELISA Kit	Thermo Fisher	BMS249-4

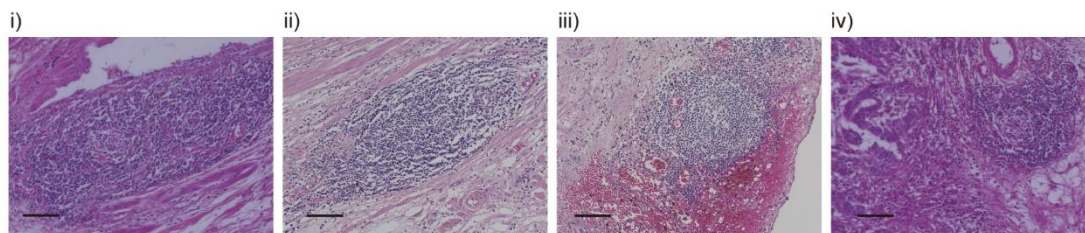
**A** Case 1



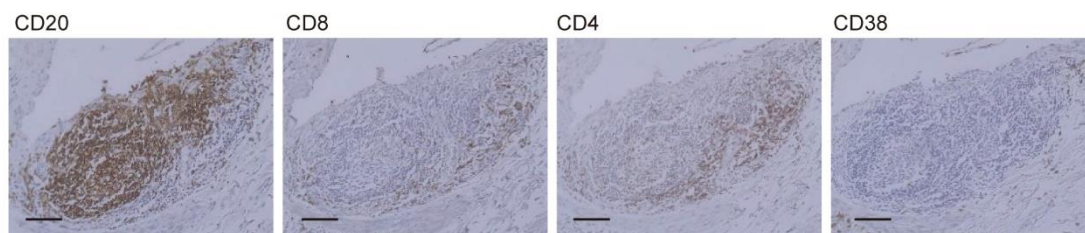
Case 2



**B**

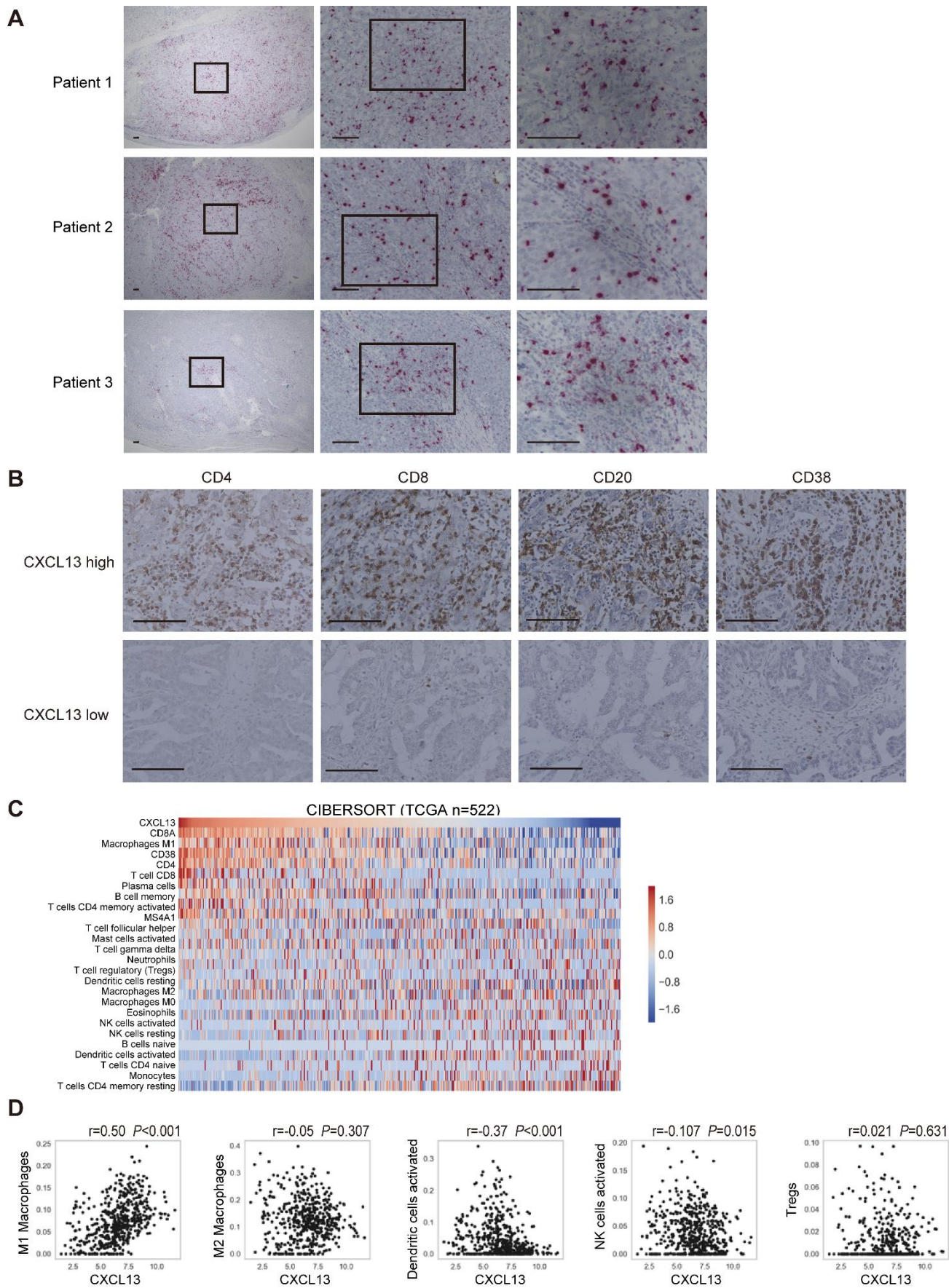


**C**



**Supplementary Figure S1. Representative TLS and dissection of TLS and tumor sites (TIL) for repertoire analysis.**

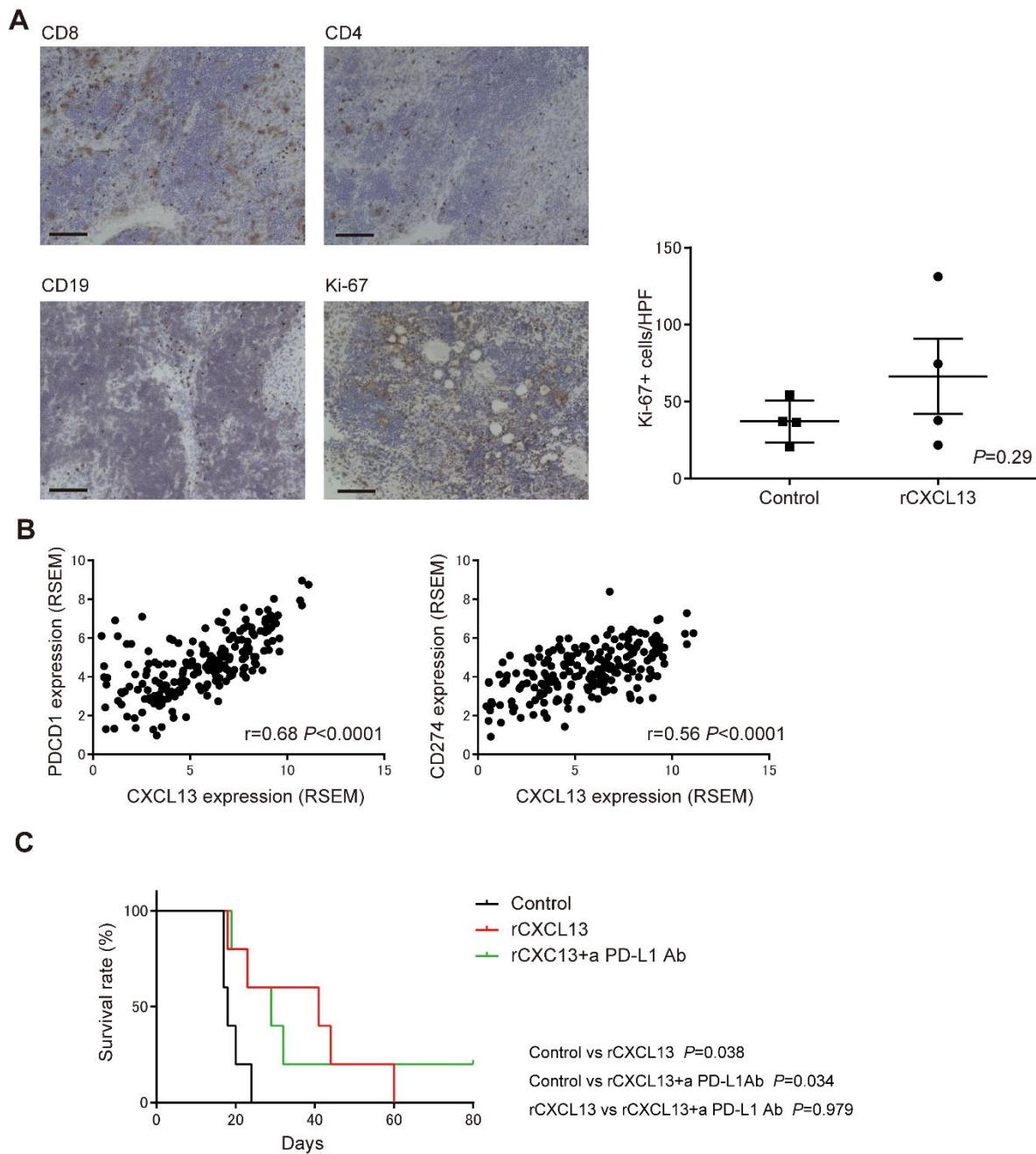
(A) As shown in the figure, the tumor area and TLS area were separated by microdissection. The tumor region was analyzed as TIL and the TLS region as TLS for repertoire analysis. (B) Representative H&E images of TLS. (C) Distribution of various lymphocytes in TLS. IHC images (DAB) of CD20, CD8, CD4, and CD38 in A(i). Scale bars indicate 1000  $\mu\text{m}$  in (A), and 100  $\mu\text{m}$  in (B) and (C).



**Supplementary Figure S2. CXCL13 expression and intratumor infiltrating lymphocytes.**

(A) CXCL13 expression in tumor infiltrating immune cells by RNA ISH (Fast RED). Representative three cases with a high expression of CXCL13 in immune cells. Scale bars indicate 100  $\mu\text{m}$ . (B) CXCL13 gene expression and

distribution of several types of tumor-infiltrating immune cells. The upper row shows a case with high CXCL13 gene expression and the lower row shows a case with low CXCL13 gene expression. Scale bars indicate 100  $\mu\text{m}$ . **(C)** The distribution of infiltrating immune cells into the tumor site and CXCL13 gene expression using CIBERSORT (n=522). Overall view of the image shown in Figure 2D. **(D)** Correlation of CXCL13 gene expression with M1- or M2-macrophages, activated dendritic cells, activated natural killer cells, or regulatory T cells (Tregs) in CIBERSORT. Correlation was determined by Spearman's correlation test.



**Supplementary Figure S3. Anti-tumor immunological effects of CXCL13 in a mouse ovarian cancer model**

(A) Analysis of cells in the TLS induced by rCXCL13 in mice by IHC of CD8, CD4, CD19, and Ki-67 (DAB). Scale bars indicate 100  $\mu\text{m}$ . The number of Ki-67 positive cells (mean count of five sections at high power field) in TLS was compared between the rCXCL13 treated group and the control group. Data are shown as the mean  $\pm$  SEM of four samples. Statistical significance was determined by two-tailed Student's *t*-test. (B) Correlation between CXCL13 and PD-1 (PDCD1) or PD-L1 (CD274) expression in TCGA ( $n=217$ ). Correlation was determined by Spearman's correlation test. (C) Survival curves of tumor-bearing mice treated with rCXCL13 or rCXCL13 + anti-PD-L1 antibodies. Analyses were performed using Kaplan-Meier estimates and log-rank tests. a PD-L1 Ab indicates anti PD-L1 antibody in (C).